

# A facile route to prepare hierarchical magnetic cobalt–silica hollow nanospheres with tunable shell thickness

Jun Wang · Chuan Hui Xu · Min Yao ·  
Jie Chen · Gao Jie Xu

Received: 14 February 2009 / Accepted: 1 July 2009 / Published online: 24 July 2009  
© Springer Science+Business Media B.V. 2009

**Abstract** Magnetic nanoshells composed of close-packed cobalt–silica nanoparticles have been successfully fabricated on silica spheres. The synthesis is facile and no high pressure, high temperature, or other severe reaction conditions were required. TEM images showed that two batches of the hollow-structured products have a good spherical morphology with an average diameter of 380 and 550 nm, respectively. The surface area and magnetic properties of cobalt–silica nanoshells are measured. By varying the times of the precipitation procedure, the shell thickness is successfully controlled within the 5–30 nm range and each time of procedure might increase the thickness about 5 nm. It is expected that the in situ reaction method can be extended to the synthesis of other hollow metal spheres. The prepared microcapsule with controllable shell thickness and interspaces has the potential to be used for controlled release applications.

**Keywords** Nanosells · Controllable · Cobalt–silica · Magnetic properties · Nanoparticles

## Introduction

In recent years, nanoscale monodisperse magnetic particles have been attracting increasing attention because of their applications in different fields, such as data storage, catalysis in chemical engineering, diagnosis of diseases, and biomolecule target delivery (Sun et al. 2000; OHandley 1999; Kim et al. 2001; Pankhurst et al. 2003). Among the different magnetic nanomaterials, hollow spheres with magnetic properties, are generally of great interest due to their wide spectrum of applications, such as controlled release capsules, nanoreactor, high-density magnetic recording, photonic crystals, and biotechnology (Caruso et al. 1998; Brune et al. 1998; Mann and Ozin 1996; Kim et al. 1998).

In respect of biomedical applications, one can combine diagnosis and controlled release in single system through filling the hollow core with desirable drugs. In particular, these magnetic hollow spheres carrying important materials outside or inside can be driven by external magnetic fields to deliver the load to certain sites, which offers a high potential application in the design of a targeting drug-delivery system (Caruso et al. 2001; Valtchev 2002; Peng et al. 2003). Therefore, a great deal of effort has been dedicated to the synthetic method of magnetic hollow spheres with desirable structure and properties.

The synthesis of the hollow spheres often relies on templating approaches, in which hard or soft sacrificial templates were used to create a hollow structure.

J. Wang (✉) · C. H. Xu · M. Yao · J. Chen  
Faculty of Science, NingBo University,  
Ningbo 315211, China  
e-mail: wjnaf@ustc.edu

J. Wang · G. J. Xu  
Ningbo Institute of Material Technology and Engineering,  
Ningbo 315201, China

Considerable effort has been devoted to the design and the controlled fabrication of magnetic hollow spheres (Bao et al. 2003; Berkowitz et al. 2004; Jin et al. 2004; Peng and Sun 2007), such as hematite and maghemite hollow spheres. For example, Peng et al. (Peng and Sun 2007) reported a solution-phase synthesis of monodisperse hollow Fe<sub>3</sub>O<sub>4</sub> nanoparticles by a controlled oxidation of Fe–Fe<sub>3</sub>O<sub>4</sub> nanoparticles with 10-nm size. In the process of the oxidation, the oxygen-transfer reagent, trimethylamine *N*-oxide (Me<sub>3</sub>NO), led to the formation of hollow structure at 210 °C. Importantly, for hollow spheres, creating tunable shell thickness may bring another dimension to tune the properties and function of nanospheres, which leads to many additional applications, such as the controlled release and catalyst applications. However, finding a general method to fabricate magnetic hollow spheres with tunable shell thickness remains a challenge. The exploration of magnetic nano-hollow spheres in function and application sectors requires a convenient, flexible, and low-cost method to prepare tailorable nanoscale magnetic hollow particles with small size and uniform morphology.

In this study, we report a novel approach of fabricating cobalt–silica magnetic hollow spheres through the hard template process. Co<sub>3</sub>(Si<sub>2</sub>O<sub>5</sub>)<sub>2</sub>(OH)<sub>2</sub>–SiO<sub>2</sub> core/shell precursor spheres are formed first on the silica sphere by a controlled surface precipitation, and then the core is removed by chemical means, and subsequently the cobalt ions are reduced by H<sub>2</sub>. The method has several advantages in the fabrication of hollow spheres; the size of hollow spheres can be adjusted by the size of core silica particles, and the shell thickness of magnetic hollow spheres can be controlled by adjusting reaction parameters. The magnetic properties of the sample of cobalt–silica shells are measured. The microporous structures present in these sphere shells can find the potential applications in the design of a targeting drug-delivery system.

## Experimental section

The monodisperse cobalt hollow spheres were synthesized by a coprecipitation of cobalt hydroxide gels in the presence of silica spheres followed by a reduction procedure. The monodisperse silica nanospheres were prepared according to the procedure described by Stöber et al. (1968; Richardson and Dubus 1978). In

the experiment, the concentrations of cobalt nitrate, urea, and SiO<sub>2</sub> monodisperse spheres (two kinds SiO<sub>2</sub> spheres with average diameter 320 nm, and 500 nm, respectively) were 0.14 M, 0.42 M, and 0.75 g/L, respectively. The mixture (200 mL) was stirred mildly at a constant temperature of 95 °C for 5 h for a complete precipitation. In order to obtain shells with the desired thickness on silica cores, the process could be repeated several times. The precipitate was dunked by NaOH (1 mol/L) to remove the core, filtered, and washed by hot distilled water. After being dried in a vacuum stove and crushed, these powders were reduced in H<sub>2</sub> current (60 cm<sup>3</sup>/min) at 650 °C (at a rate of 10 °C/min) for 3 h in the fixed-bed reactor. After the completion of the reduction process, the sample was outgassed in purified argon for 1 h at 30 °C above the reduction temperature to remove the absorbed hydrogen. It was then cooled to ambient temperature in the flowing-inert gas. In order to maintain the spherical shape of the shell, the concentration of strong base should be carefully controlled to avoid the damage of the shell. Because of the support of the core, the shell did not collapse when these powders were dispersed by the ultrasound. After the reduction, the morphology of the shells remained to be the same as that before the reduction reaction.

Structural characterization of the samples was performed by means of X-ray diffraction (XRD) using a diffractometer (D/Max-γA) with Co radiation ( $\lambda = 1.7889 \text{ \AA}$ ). The morphology of the sample was measured using a field emission scanning electron microscope (Hitachi S-4800) and a transmission electron microscope (TEM) with a Tecnai G2 F20, using an accelerating voltage of 200 kV. BET surface area was obtained by analyzing N<sub>2</sub> adsorption/desorption isotherm data and from Micromeritics (ASAP 2020M) measurement. The magnetic properties were evaluated on a PPMS-9 at room temperature, and the saturation magnetic field reached 8 T.

## Results and discussion

The crystal structure of magnetic hollow spheres was identified from the X-ray diffraction pattern (Fig. 1). The result of Fig. 1 reveals that the samples are composed of cobalt–silica, and the XRD diffraction patterns of cobalt are in good accordance with the American Society for Testing and Materials standard

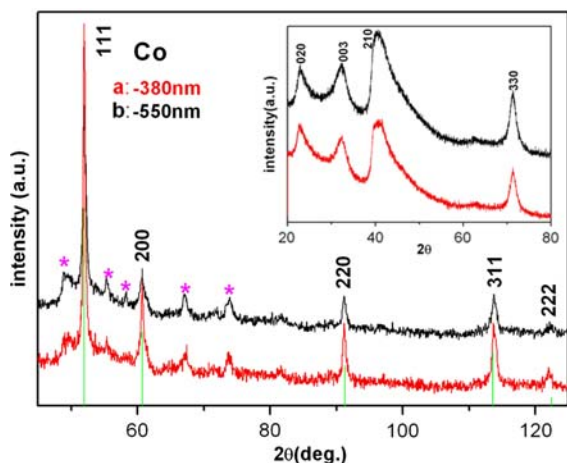


**Fig. 1** XRD patterns of different nanospheres: (a) 380 nm and (b) 550 nm cobalt–silica hollow sphere reduced at 650 °C after removing the silica core. Asterisk symbol shows the mixture of the cobalt–silica. The inset is as-prepared silica complexes  $[\text{Co}_3(\text{Si}_2\text{O}_5)_2(\text{OH})_2]$  spheres calcined at 450 °C

(JCPDS 01-1255). X-ray diffraction patterns in the inset of Fig. 1 show that as-prepared silica spheres deposited with  $\text{Co}^{2+}$  ions are cobalt antigorite (structural formula  $\text{Co}_3(\text{Si}_2\text{O}_5)_2(\text{OH})_2$  JCPDS 21-0871). The method used in this article consists of the precipitation of a cobalt (II) phase onto the silica spheres by the basification of a cobalt salt solution. The same result has been reported by Richardson (Richardson and Dubus 1978). The key factor of this preparation is the basification, i.e., the gradual and homogeneous generation of hydroxide ions throughout the whole solution, to avoid locally high pH, and the subsequent precipitation of cobalt hydroxide in the solution. The use of urea ( $\text{CO}(\text{NH}_2)_2$ ) rather than sodium hydroxide is advised because the solution mixing and the basification can be performed in two separate steps: urea is mixed to the solution at room temperature, and urea hydrolysis starts when the mixture is heated at 95 °C: hydroxide ions are homogeneously generated within the solution (Shaw and Bordeaux 1955).

Figure 2 shows the TEM and SEM images of the monodisperse cobalt–silica spheres. In Fig. 2a, the dark regions can be seen in the central parts of the spheres, in contrast to the pale edges, indicating a spherical core–shell structure (silica– $\text{Co}_3(\text{Si}_2\text{O}_5)_2(\text{OH})_2$ ) with uniform sizes in both diameter and shell thickness. The image in Fig. 2b also shows that these shells are also porous, which is much different from the smooth surface of the

bare silica nanospheres. The nanoshell phase did not bind the silica core tightly. Because of the formation of a new compound of  $\text{Co}_3(\text{Si}_2\text{O}_5)_2(\text{OH})_2$  on the core–shell interface, the shells began to separate from the cores with increasing thickness of the shells.

The morphology and the shell thickness of the cobalt hollow spheres were further examined by TEM. Figure 2c shows that the morphology of magnetic hollow spheres did not change significantly after the  $\text{SiO}_2$  cores were removed and the resulting shells were treated with  $\text{H}_2$ . The magnetic sample possesses uniform shell thickness with a total shell thickness of about 30 nm after precipitations for six times. Because of the ultrasonic treatment of sample for TEM examination, some magnetic hollow spheres are broken, which also confirm that the spheres are hollow.

In order to control the shell thickness of the hollow nanospheres, the reaction time was varied while the concentration of each reactant in the precipitation reaction was kept unchanged. One representative product (precipitation reactions repeated three times) in the inset of Fig. 2d was obtained to demonstrate the ease in controlling the shell thickness. The thickness of nanoshell can be varied by the number of coating, and each coating increases the thickness by about 5 nm.

In Fig. 3a, a HRTEM image obtained from a portion of an individual cobalt–silica composite reveals that the shells are composed of sheet-like structure of 3-nm thickness integrating closely to form a uniform layer. In order to confirm the chemical composition of the as-prepared structures, EDS spectra (Fig. 3b) were taken at the selected positions of the sample. The elemental signatures obtained are identical within experimental accuracy, and essentially only Co, Si, and O, were observed, as expected. We note that the relative intensity of Co:Si:O is 7:5:10. The Cu and C signals arise from the TEM grid.

Nitrogen adsorption and desorption analysis was further employed to investigate the pore structure of the cobalt hollow spheres (inset of Fig. 4). The pore size distribution is centered at 3.9 nm (380-nm spheres) and 3.8 nm (550-nm spheres) calculated from the desorption branch by the Barrett–Joyner–Halenda (BJH) method (Fig. 4), which agrees well with the inner diameter of the needlelike structure observed by TEM. The BET surface area of the 380-nm sample is about 206  $\text{cm}^2/\text{g}$ , which is about the same as that of 550 nm of sample (204  $\text{cm}^2/\text{g}$ ). The pore volumes of

**Fig. 2** TEM (a) and SEM (b) images of silica– $\text{Co}_3(\text{Si}_2\text{O}_5)_2(\text{OH})_2$  core–shell structure; TEM images of c cobalt hollow spheres with 30-nm shell thickness and d higher magnification; the inset image is cobalt hollow sphere with 15-nm shell thickness after precipitant reactions repeated three times

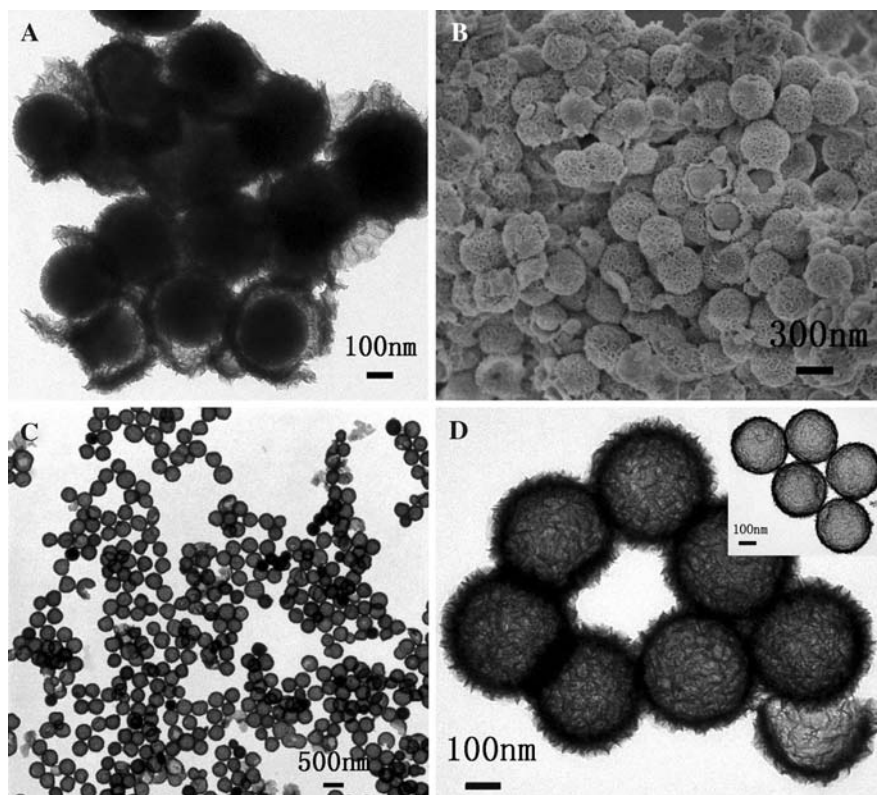
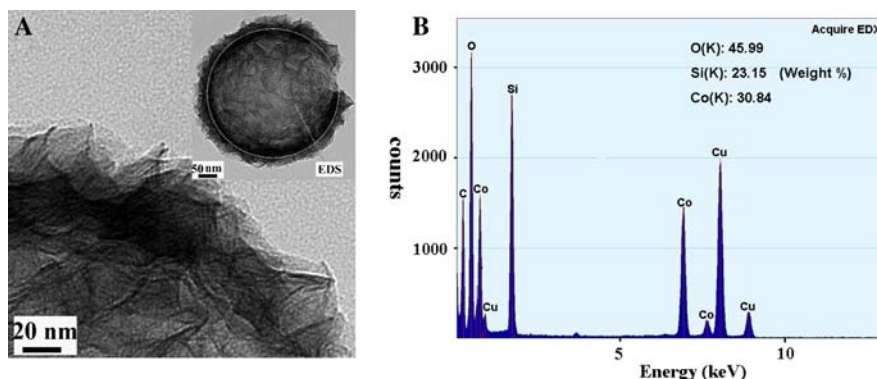


**Fig. 3** The high magnification TEM images of a magnetic cobalt–silica hollow spheres; the inset TEM image of individual hollow sphere and b DEX spectra obtained from the individual cobalt–silica hollow sphere. The Cu and C peaks originate from the TEM grid



the 550 and 380 nm magnetic hollow spheres are 0.201 mL/g and 0.19 mL/g, respectively. A majority of the pores have a diameter <4 nm, which might exist in silica matrix; other pores with bigger sizes might come from the aggregates of Co nanoparticles.

The magnetic properties of Co nanoshells are measured using a vibrating sample magnetometer at room temperature. The hysteresis loop is displayed in Fig. 5. The superparamagnetic behavior is observed for the sample at room temperature. The saturation magnetization ( $M_s$ ) of the cobalt–silica nanoshell is 32.8 and 31.1 emu/g for 380-nm and 550-nm spheres,

respectively, lower than the reported value for bulk Co (168 emu/g) (Dumpich et al. 2002). The saturation magnetization of magnetic nanoparticles is found to be much smaller than the bulk value and decreases with the decreasing of the particle size. For nanoparticles, the main reasons resulting in decrease of  $M_s$  may come from the nature of ultrafine particles, surface disorder, and cation distribution. For our sample, the main reason may be that the hollow sphere is a compound of cobalt–silica, not pure cobalt. The silica compound layer could serve as a non-magnetic layer and reduce cobalt proportion of cobalt–silica



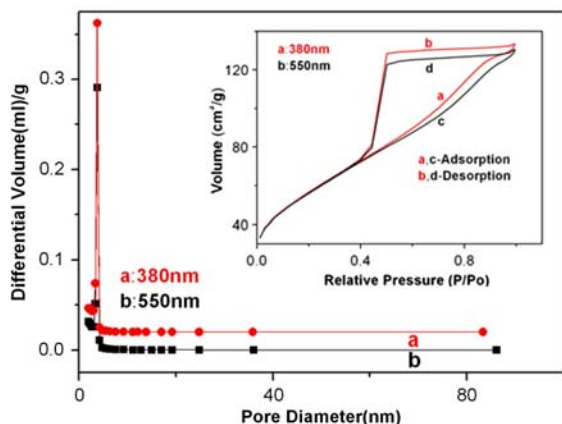


**Fig. 4** The pore diameter distribution and the inset of  $N_2$  adsorption/desorption isotherm of cobalt hollow spheres (550 and 380 nm)

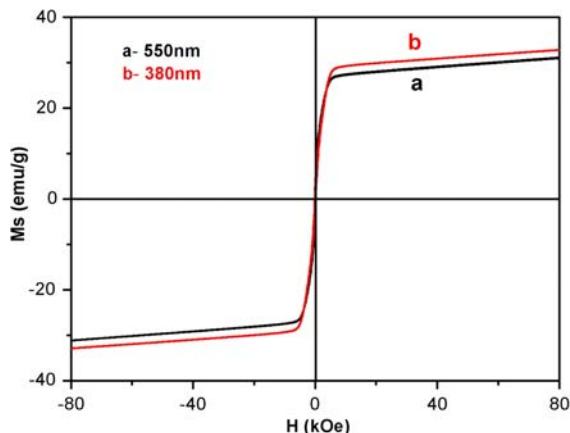


**Fig. 5** Magnetic hysteresis curves of Co hollow spheres with 380- and 550-nm diameter. The measurement was carried out at room temperature

compound, which results in the decrease of saturation magnetization. The phenomena have been observed in several magnetic materials system (Sato et al. 1987; van der Zaag et al. 1993; Berkowitz et al. 1987). The existence of the nonmagnetic layer might be caused by the canting of the surface spins (Coey 1971), a high anisotropy layer, or the loss of the long-range order in the surface layer (Berkowitz and Walter 1982).

## Conclusion

Silica colloidal spheres were successfully used as source of silicate ions as well as templates in the

synthesis of hierarchical cobalt–silica hollow spheres via the reduction of  $Co^{2+}$  on silica spheres. The physical characterization and the magnetic properties have been investigated. The formation mechanism of sheetlike structure is that the generated cobalt silicate grows in situ around the silica colloidal spheres. The prepared hollow spheres with controllable shell thickness and interspace have the potential to be used for controlled release applications. The hierarchical cobalt–silica hollow spheres exhibited large specific surface area and superparamagnetism at room temperature. The synthesis procedure is facile and this simple in situ reaction method will promote the development of new superstructures.

**Acknowledgments** This study was supported by the National Natural Science Foundation of China (10874095), the Natural Science Foundation of China, Zhe Jiang (Y407267), the Natural Science Foundation of Ningbo (2008A610042 and 2008B10051), and K. C. Wong Magna Foundation in Ningbo University.

## References

- Bao JC, Liang YY, Xu Z, Si L (2003) Facile synthesis of hollow nickel submicrometer spheres. *Adv Mater* 15: 1832–1835
- Berkowitz AE, Walter JL (1982) Amorphous particles produced by spark erosion. *Mater Sci Eng* 55:275–287
- Berkowitz AE, Schuele WJ, Flanders PJ (1987) Influence of crystallite size on the magnetic properties of acicular  $\gamma$ - $Fe_2O_3$  particles. *J Appl Phys* 39:1261–1263
- Berkowitz AE, Harper H, Smith DJ, Hu H, Jiang Q, Solomon VC, Radosky HB (2004) Hollow metallic microspheres produced by spark erosion. *Appl Phys Lett* 85:940–942
- Brune H, Giovannini M, Bromann K, Kern K (1998) Self-organized growth of nanostructure arrays on strain-relief patterns. *Nature* 394:451–452
- Caruso F, Caruso RA, Mohwald H (1998) “Green Rust” in the lab and in the soil. *Science* 282:1111
- Caruso RA, Schattka JH, Greiner A (2001) Titanium dioxide tubes from sol-gel coating of electrospun polymer fibers. *Adv Mater* 13:1577–1579
- Coey JMD (1971) Noncollinear spin arrangement in ultrafine ferrimagnetic crystallites. *Phys Rev Lett* 27:1140–1142
- Dumpich G, Krome TP, Hausmans B (2002) Magnetoresistance of single Co nanowires. *J Magn Magn Mater* 248:241–247
- Jin P, Chen QW, Hao LQ (2004) Synthesis and catalytic properties of nickel–silica composite hollow nanospheres. *J Phys Chem B* 108:6311–6314
- Kim SS, Zhang W, Pinnavaia TJ (1998) Ultrastable mesostructured silica vesicles. *Science* 282:1302–1305
- Kim DK, Zhang Y, Kehr J, Klason T, Bjelke B, Muhammed MJ (2001) Characterization and MRI study of surfactant-coated superparamagnetic nanoparticles administered into the rat brain. *J Magn Magn Mater* 225:256–261

- Mann S, Ozin GA (1996) Synthesis of inorganic materials with complex form. *Nature* 382:313–318
- OHandley RC (1999) *Modern magnetic materials*. Wiley, New York
- Pankhurst QA, Connolly J, Dobson J (2003) Applications of magnetic nanoparticles in biomedicine. *J Phys D* 36: R167–R181
- Peng S, Sun SH (2007) Synthesis and characterization of hollow Fe<sub>3</sub>O<sub>4</sub> nanoparticles. *Angew Chem Int Ed Engl* 46:4155–4158
- Peng Q, Dong Y, Li Y (2003) ZnSe semiconductor hollow microspheres. *Angew Chem Int Ed Engl* 42:3027–3030
- Richardson JT, Dubus RJ (1978) Preparation variables in nickel catalysts. *J Catal* 54:207–218
- Sato T, Iijima T, Seki M, Inagaki N (1987) Magnetic properties of ultrafine ferrite particles. *J Magn Magn Mater* 65:252–256
- Shaw WHR, Bordeaux JJ (1955) The decomposition of urea in aqueous media. *J Am Chem Soc* 77:4729–4733
- Stöber W, Fink A, Bohn E (1968) Controlled growth of monodisperse silica spheres in the micron size range. *J Colloid Interface Sci* 26:62–69
- Sun S, Murray CB, Weller D, Folks L, Moser A (2000) Monodisperse FePt nanoparticles and ferromagnetic FePt nanocrystal superlattices. *Science* 287:1989–1992
- Valtchev V (2002) Core–shell polystyrene/zeolite A microbeads. *Chem Mater* 14:956–958
- van der Zaag PJ, Ruigrok JJM, Noordermeer A, van Delden MHMW, Por PT, Rekveldt MTH, Donnet DM, Chapman JN (1993) The initial permeability of polycrystalline MnZn ferrites: the influence of domain and microstructure. *J Appl Phys* 74:4085–4095